BABAR-PUB-01/23
SLAC-PUB-9065

Direct CP Violation Searches in Charmless Hadronic B Meson Decays

B. Aubert,[1] D. Boutigny,[1] J.-M. Gaillard,[1] A. Hicheur,[1] Y. Karyotakis,[1] J. P. Lees,[1] P. Robbe,[1] V. Tisserand,[1] A. Palano,[2] A. Pompili,[2] G. P. Chen,[3] J. C. Chen,[3] N. D. Qi,[3] G. Rong,[3] P. Wang,[3] Y. S. Zhu,[3] G. Eigen,[4] B. Stugu,[4] G. S. Abrams,[5] A. W. Borgland,[5] A. B. Breon,[5] D. N. Brown,[5] J. Button-Shafer,[5] R. N. Cahn,[5] A. R. Clark,[5] M. S. Gill,[5] A. V. Gritsan,[5] Y. Groysman,[5] R. G. Jacobsen,[5] R. W. Kadel,[5] J. Kadyk,[5] L. T. Kerth,[5] Yu. G. Kolomensky,[5] J. F. Kral,[5] C. LeClerc,[5] M. E. Levi,[5] G. Lynch,[5] P. J. Oddone,[5] M. Pripstein,[5] N. A. Roe,[5] A. Romosan,[5] M. T. Ronan,[5] V. G. Shelkov,[5] A. V. Telnov,[5] W. A. Wenzel,[5] P. G. Bright-Thomas,[6] T. J. Harrison,[6] C. M. Hawkes,[6] D. J. Knowles,[6] S. W. O'Neale,[6] R. C. Penny,[6] A. T. Watson,[6] N. K. Watson,[6] T. Deppermann,[7] K. Goetzen,[7] H. Koch,[7] M. Kunze,[7] B. Lewandowski,[7] K. Peters,[7] H. Schmuecker,[7] M. Steinke,[7] N. R. Barlow,[8] W. Bhimji,[8] N. Chevalier,[8] P. J. Clark,[8] W. N. Cottingham,[8] B. Foster,[8] C. Mackay,[8] F. F. Wilson,[8] K. Abe,[9] C. Hearty,[9] T. S. Mattison,[9] J. A. McKenna,[9] D. Thiessen,[9] S. Jolly,[10] A. K. McKemey,[10] V. E. Blinov,[11] A. D. Bukin,[11] D. A. Bukin,[11] A. R. Buzykaev,[11] V. B. Golubev,[11] V. N. Ivanchenko,[11] A. A. Korol,[11] E. A. Kravchenko,[11] A. P. Onuchin,[11] S. I. Serednyakov,[11] Yu. I. Skovpen,[11] V. I. Telnov,[11] A. N. Yushkov,[11] D. Best,[12] M. Chao,[12] D. Kirkby,[12] A. J. Lankford,[12] M. Mandelkern,[12] S. McMahon,[12] D. P. Stoker,[12] K. Arisaka,[13] C. Buchanan,[13] S. Chun,[13] D. B. MacFarlane,[14] S. Prell,[14] Sh. Rahatlou,[14] G. Raven,[14] V. Sharma,[14] C. Campagnari,[15] B. Dahmes,[15] P. A. Hart,[15] N. Kuznetsova,[15] S. L. Levy,[15] O. Long,[15] A. Lu,[15] J. D. Richman,[15] W. Verkerke,[15] J. Beringer,[16] A. M. Eisner,[16] M. Grothe,[16] C. A. Heusch,[16] W. S. Lockman,[16] T. Pulliam,[16] T. Schalk,[16] R. E. Schmitz,[16] B. A. Schumm,[16] A. Seiden,[16] M. Turri,[16] W. Walkowiak,[16] D. C. Williams,[16] M. G. Wilson,[16] E. Chen,[17] G. P. Dubois-Felsmann,[17] A. Dvoretskii,[17] D. G. Hitlin,[17] S. Metzler,[17] J. Oyang,[17] F. C. Porter,[17] A. Ryd,[17] A. Samuel,[17] M. Weaver,[17] S. Yang,[17] R. Y. Zhu,[17] S. Devmal,[18] T. L. Geld,[18] S. Jayatilleke,[18] G. Mancinelli,[18] B. T. Meadows,[18] M. D. Sokoloff,[18] T. Barillari,[19] P. Bloom,[19] M. O. Dima,[19] W. T. Ford,[19] U. Nauenberg,[19] A. Olivas,[19] P. Rankin,[19] J. Roy,[19] J. G. Smith,[19] W. C. van Hoek,[19] J. Blouw,[20] J. L. Harton,[20] M. Krishnamurthy,[20] A. Soffer,[20] W. H. Toki,[20] R. J. Wilson,[20] J. Zhang,[20] T. Brandt,[21] J. Brose,[21] T. Colberg,[21] M. Dickopp,[21] R. S. Dubitzky,[21] A. Hauke,[21] E. Maly,[21] R. Müller-Pfefferkorn,[21] S. Otto,[21] K. R. Schubert,[21] R. Schwierz,[21] B. Spaan,[21] L. Wilden,[21] D. Bernard,[22] G. R. Bonneaud,[22] F. Brochard,[22] J. Cohen-Tanugi,[22] S. Ferrag,[22] S. T'Jampens,[22] Ch. Thiebaux,[22] G. Vasileiadis,[22] M. Verderi,[22] A. Anjomshoaa,[23] R. Bernet,[23] A. Khan,[23] D. Lavin,[23] F. Muheim,[23] S. Playfer,[23] J. E. Swain,[23] J. Tinslay,[23] M. Falbo,[24] C. Borean,[25] C. Bozzi,[25] L. Piemontese,[25] E. Treadwell,[26] F. Anulli,[27,*] R. Baldini-Ferroli,[27] A. Calcaterra,[27] R. de Sangro,[27] D. Falciai,[27] G. Finocchiaro,[27] P. Patteri,[27] I. M. Peruzzi,[27,*] M. Piccolo,[27] Y. Xie,[27] A. Zallo,[27] S. Bagnasco,[28] A. Buzzo,[28] R. Contri,[28] G. Crosetti,[28] M. Lo Vetere,[28] M. Macri,[28] M. R. Monge,[28] S. Passaggio,[28] F. C. Pastore,[28] C. Patrignani,[28] M. G. Pia,[28] E. Robutti,[28] A. Santroni,[28] S. Tosi,[28] M. Morii,[29] R. Bartoldus,[30] R. Hamilton,[30] U. Mallik,[30] J. Cochran,[31] H. B. Crawley,[31] P.-A. Fischer,[31] J. Lamsa,[31] W. T. Meyer,[31] E. I. Rosenberg,[31] G. Grosdidier,[32] C. Hast,[32] A. Höcker,[32] H. M. Lacker,[32] S. Laplace,[32] V. Lepeltier,[32] A. M. Lutz,[32] S. Plaszczynski,[32] M. H. Schune,[32] S. Trincaz-Duvoid,[32] G. Wormser,[32] R. M. Bionta,[33] V. Brigljević,[33] D. J. Lange,[33] M. Mugge,[33] K. van Bibber,[33] D. M. Wright,[33] A. J. Bevan,[34] J. R. Fry,[34] E. Gabathuler,[34] R. Gamet,[34] M. George,[34] M. Kay,[34] D. J. Payne,[34] R. J. Sloane,[34] C. Touramanis,[34] M. L. Aspinwall,[35] D. A. Bowerman,[35] P. D. Dauncey,[35] U. Egede,[35] I. Eschrich,[35] N. J. W. Gunawardane,[35] J. A. Nash,[35] P. Sanders,[35] D. Smith,[35] D. E. Azzopardi,[36] J. J. Back,[36] P. Dixon,[36] P. F. Harrison,[36] R. J. L. Potter,[36] H. W. Shorthouse,[36] P. Strother,[36] P. B. Vidal,[36] G. Cowan,[37] S. George,[37] M. G. Green,[37] A. Kurup,[37] C. E. Marker,[37] P. McGrath,[37] T. R. McMahon,[37] S. Ricciardi,[37] F. Salvatore,[37] G. Vaitsas,[37] D. Brown,[38] C. L. Davis,[38] J. Allison,[39] R. J. Barlow,[39] J. T. Boyd,[39] A. C. Forti,[39] J. Fullwood,[39] F. Jackson,[39] G. D. Lafferty,[39] N. Savvas,[39] J. H. Weatherall,[39] J. C. Williams,[39] A. Farbin,[40] A. Jawahery,[40] V. Lillard,[40] J. Olsen,[40] D. A. Roberts,[40] J. R. Schieck,[40] G. Blaylock,[41] C. Dallapiccola,[41] K. T. Flood,[41] S. S. Hertzbach,[41] R. Kofler,[41] V. G. Koptchev,[41] T. B. Moore,[41] H. Staengle,[41] S. Willocq,[41] B. Brau,[42] R. Cowan,[42] G. Sciolla,[42] F. Taylor,[42] R. K. Yamamoto,[42] M. Milek,[43] P. M. Patel,[43] F. Palombo,[44] J. M. Bauer,[45] L. Cremaldi,[45] V. Eschenburg,[45] R. Kroeger,[45] J. Reidy,[45] D. A. Sanders,[45] D. J. Summers,[45] J. Y. Nief,[46] P. Taras,[46] H. Nicholson,[47] C. Cartaro,[48] N. Cavallo,[48,†] G. De Nardo,[48] F. Fabozzi,[48] C. Gatto,[48] L. Lista,[48] P. Paolucci,[48]

D. Piccolo,[48] C. Sciacca,[48] J. M. LoSecco,[49] J. R. G. Alsmiller,[50] T. A. Gabriel,[50] T. Handler,[50] J. Brau,[51]
R. Frey,[51] E. Grauges,[51] M. Iwasaki,[51] N. B. Sinev,[51] D. Strom,[51] F. Colecchia,[52] F. Dal Corso,[52] A. Dorigo,[52]
F. Galeazzi,[52] M. Margoni,[52] G. Michelon,[52] M. Morandin,[52] M. Posocco,[52] M. Rotondo,[52] F. Simonetto,[52]
R. Stroili,[52] E. Torassa,[52] C. Voci,[52] M. Benayoun,[53] H. Briand,[53] J. Chauveau,[53] P. David,[53] Ch. de la Vaissière,[53]
L. Del Buono,[53] O. Hamon,[53] F. Le Diberder,[53] Ph. Leruste,[53] J. Ocariz,[53] L. Roos,[53] J. Stark,[53] P. F. Manfredi,[54]
V. Re,[54] V. Speziali,[54] E. D. Frank,[55] L. Gladney,[55] Q. H. Guo,[55] J. Panetta,[55] C. Angelini,[56] G. Batignani,[56]
S. Bettarini,[56] M. Bondioli,[56] E. Campagna,[56] M. Carpinelli,[56] F. Forti,[56] M. A. Giorgi,[56] A. Lusiani,[56]
F. Martinez-Vidal,[56] M. Morganti,[56] N. Neri,[56] E. Paoloni,[56] M. Rama,[56] G. Rizzo,[56] F. Sandrelli,[56] G. Simi,[56]
G. Triggiani,[56] J. Walsh,[56] M. Haire,[57] D. Judd,[57] K. Paick,[57] L. Turnbull,[57] D. E. Wagoner,[57] J. Albert,[58]
P. Elmer,[58] C. Lu,[58] V. Miftakov,[58] S. F. Schaffner,[58] A. J. S. Smith,[58] A. Tumanov,[58] E. W. Varnes,[58]
G. Cavoto,[59] D. del Re,[59] R. Faccini,[14, 59] F. Ferrarotto,[59] F. Ferroni,[59] E. Lamanna,[59] M. A. Mazzoni,[59]
S. Morganti,[59] G. Piredda,[59] F. Safai Tehrani,[59] M. Serra,[59] C. Voena,[59] S. Christ,[60] R. Waldi,[60] T. Adye,[61] N. De
Groot,[61] B. Franek,[61] N. I. Geddes,[61] G. P. Gopal,[61] S. M. Xella,[61] R. Aleksan,[62] S. Emery,[62] A. Gaidot,[62]
S. F. Ganzhur,[62] P.-F. Giraud,[62] G. Hamel de Monchenault,[62] W. Kozanecki,[62] M. Langer,[62] G. W. London,[62]
B. Mayer,[62] B. Serfass,[62] G. Vasseur,[62] Ch. Yèche,[62] M. Zito,[62] M. V. Purohit,[63] H. Singh,[63] A. W. Weidemann,[63]
F. X. Yumiceva,[63] I. Adam,[64] D. Aston,[64] N. Berger,[64] A. M. Boyarski,[64] G. Calderini,[64] M. R. Convery,[64]
D. P. Coupal,[64] D. Dong,[64] J. Dorfan,[64] W. Dunwoodie,[64] R. C. Field,[64] T. Glanzman,[64] S. J. Gowdy,[64]
T. Haas,[64] T. Himel,[64] T. Hryn'ova,[64] M. E. Huffer,[64] W. R. Innes,[64] C. P. Jessop,[64] M. H. Kelsey,[64]
P. Kim,[64] M. L. Kocian,[64] U. Langenegger,[64] D. W. G. S. Leith,[64] S. Luitz,[64] V. Luth,[64] H. L. Lynch,[64]
H. Marsiske,[64] S. Menke,[64] R. Messner,[64] D. R. Muller,[64] C. P. O'Grady,[64] V. E. Ozcan,[64] A. Perazzo,[64]
M. Perl,[64] S. Petrak,[64] H. Quinn,[64] B. N. Ratcliff,[64] S. H. Robertson,[64] A. Roodman,[64] A. A. Salnikov,[64]
T. Schietinger,[64] R. H. Schindler,[64] J. Schwiening,[64] A. Snyder,[64] A. Soha,[64] S. M. Spanier,[64] J. Stelzer,[64] D. Su,[64]
M. K. Sullivan,[64] H. A. Tanaka,[64] J. Va'vra,[64] S. R. Wagner,[64] A. J. R. Weinstein,[64] W. J. Wisniewski,[64]
D. H. Wright,[64] C. C. Young,[64] P. R. Burchat,[65] C. H. Cheng,[65] T. I. Meyer,[65] C. Roat,[65] R. Henderson,[66]
W. Bugg,[67] H. Cohn,[67] J. M. Izen,[68] I. Kitayama,[68] X. C. Lou,[68] F. Bianchi,[69] M. Bona,[69] D. Gamba,[69]
L. Bosisio,[70] G. Della Ricca,[70] S. Dittongo,[70] L. Lanceri,[70] P. Poropat,[70] G. Vuagnin,[70] R. S. Panvini,[71]
C. M. Brown,[72] P. D. Jackson,[72] R. Kowalewski,[72] J. M. Roney,[72] H. R. Band,[73] E. Charles,[73] S. Dasu,[73]
A. M. Eichenbaum,[73] H. Hu,[73] J. R. Johnson,[73] R. Liu,[73] F. Di Lodovico,[73] Y. Pan,[73] R. Prepost,[73] I. J. Scott,[73]
S. J. Sekula,[73] J. H. von Wimmersperg-Toeller,[73] S. L. Wu,[73] Z. Yu,[73] T. M. B. Kordich,[74] and H. Neal[74]
(The *BABAR* Collaboration)

[1]*Laboratoire de Physique des Particules, F-74941 Annecy-le-Vieux, France*
[2]*Università di Bari, Dipartimento di Fisica and INFN, I-70126 Bari, Italy*
[3]*Institute of High Energy Physics, Beijing 100039, China*
[4]*University of Bergen, Inst. of Physics, N-5007 Bergen, Norway*
[5]*Lawrence Berkeley National Laboratory and University of California, Berkeley, CA 94720, USA*
[6]*University of Birmingham, Birmingham, B15 2TT, United Kingdom*
[7]*Ruhr Universität Bochum, Institut für Experimentalphysik 1, D-44780 Bochum, Germany*
[8]*University of Bristol, Bristol BS8 1TL, United Kingdom*
[9]*University of British Columbia, Vancouver, BC, Canada V6T 1Z1*
[10]*Brunel University, Uxbridge, Middlesex UB8 3PH, United Kingdom*
[11]*Budker Institute of Nuclear Physics, Novosibirsk 630090, Russia*
[12]*University of California at Irvine, Irvine, CA 92697, USA*
[13]*University of California at Los Angeles, Los Angeles, CA 90024, USA*
[14]*University of California at San Diego, La Jolla, CA 92093, USA*
[15]*University of California at Santa Barbara, Santa Barbara, CA 93106, USA*
[16]*University of California at Santa Cruz, Institute for Particle Physics, Santa Cruz, CA 95064, USA*
[17]*California Institute of Technology, Pasadena, CA 91125, USA*
[18]*University of Cincinnati, Cincinnati, OH 45221, USA*
[19]*University of Colorado, Boulder, CO 80309, USA*
[20]*Colorado State University, Fort Collins, CO 80523, USA*
[21]*Technische Universität Dresden, Institut für Kern- und Teilchenphysik, D-01062, Dresden, Germany*
[22]*Ecole Polytechnique, F-91128 Palaiseau, France*
[23]*University of Edinburgh, Edinburgh EH9 3JZ, United Kingdom*
[24]*Elon University, Elon University, NC 27244-2010, USA*
[25]*Università di Ferrara, Dipartimento di Fisica and INFN, I-44100 Ferrara, Italy*
[26]*Florida A&M University, Tallahassee, FL 32307, USA*

[27]Laboratori Nazionali di Frascati dell'INFN, I-00044 Frascati, Italy
[28]Università di Genova, Dipartimento di Fisica and INFN, I-16146 Genova, Italy
[29]Harvard University, Cambridge, MA 02138, USA
[30]University of Iowa, Iowa City, IA 52242, USA
[31]Iowa State University, Ames, IA 50011-3160, USA
[32]Laboratoire de l'Accélérateur Linéaire, F-91898 Orsay, France
[33]Lawrence Livermore National Laboratory, Livermore, CA 94550, USA
[34]University of Liverpool, Liverpool L69 3BX, United Kingdom
[35]University of London, Imperial College, London, SW7 2BW, United Kingdom
[36]Queen Mary, University of London, E1 4NS, United Kingdom
[37]University of London, Royal Holloway and Bedford New College, Egham, Surrey TW20 0EX, United Kingdom
[38]University of Louisville, Louisville, KY 40292, USA
[39]University of Manchester, Manchester M13 9PL, United Kingdom
[40]University of Maryland, College Park, MD 20742, USA
[41]University of Massachusetts, Amherst, MA 01003, USA
[42]Massachusetts Institute of Technology, Laboratory for Nuclear Science, Cambridge, MA 02139, USA
[43]McGill University, Montréal, QC, Canada H3A 2T8
[44]Università di Milano, Dipartimento di Fisica and INFN, I-20133 Milano, Italy
[45]University of Mississippi, University, MS 38677, USA
[46]Université de Montréal, Laboratoire René J. A. Lévesque, Montréal, QC, Canada H3C 3J7
[47]Mount Holyoke College, South Hadley, MA 01075, USA
[48]Università di Napoli Federico II, Dipartimento di Scienze Fisiche and INFN, I-80126, Napoli, Italy
[49]University of Notre Dame, Notre Dame, IN 46556, USA
[50]Oak Ridge National Laboratory, Oak Ridge, TN 37831, USA
[51]University of Oregon, Eugene, OR 97403, USA
[52]Università di Padova, Dipartimento di Fisica and INFN, I-35131 Padova, Italy
[53]Universités Paris VI et VII, Lab de Physique Nucléaire H. E., F-75252 Paris, France
[54]Università di Pavia, Dipartimento di Elettronica and INFN, I-27100 Pavia, Italy
[55]University of Pennsylvania, Philadelphia, PA 19104, USA
[56]Università di Pisa, Scuola Normale Superiore and INFN, I-56010 Pisa, Italy
[57]Prairie View A&M University, Prairie View, TX 77446, USA
[58]Princeton University, Princeton, NJ 08544, USA
[59]Università di Roma La Sapienza, Dipartimento di Fisica and INFN, I-00185 Roma, Italy
[60]Universität Rostock, D-18051 Rostock, Germany
[61]Rutherford Appleton Laboratory, Chilton, Didcot, Oxon, OX11 0QX, United Kingdom
[62]DAPNIA, Commissariat à l'Energie Atomique/Saclay, F-91191 Gif-sur-Yvette, France
[63]University of South Carolina, Columbia, SC 29208, USA
[64]Stanford Linear Accelerator Center, Stanford, CA 94309, USA
[65]Stanford University, Stanford, CA 94305-4060, USA
[66]TRIUMF, Vancouver, BC, Canada V6T 2A3
[67]University of Tennessee, Knoxville, TN 37996, USA
[68]University of Texas at Dallas, Richardson, TX 75083, USA
[69]Università di Torino, Dipartimento di Fiscia Sperimentale and INFN, I-10125 Torino, Italy
[70]Università di Trieste, Dipartimento di Fisica and INFN, I-34127 Trieste, Italy
[71]Vanderbilt University, Nashville, TN 37235, USA
[72]University of Victoria, Victoria, BC, Canada V8W 3P6
[73]University of Wisconsin, Madison, WI 53706, USA
[74]Yale University, New Haven, CT 06511, USA

(Dated: June 22, 2011)

We search for direct CP violation in charmless hadronic B decays observed in a sample of about 22.7 million $B\overline{B}$ pairs collected with the *BABAR* detector at the PEP-II asymmetric-energy e^+e^- collider. We measure the following charge asymmetries: $\mathcal{A}_{CP}(B^\pm \to \eta' K^\pm) = -0.11 \pm 0.11 \pm 0.02$, $\mathcal{A}_{CP}(B^\pm \to \omega\pi^\pm) = -0.01 \,^{+\,0.29}_{-\,0.31} \pm 0.03$, $\mathcal{A}_{CP}(B^\pm \to \phi K^\pm) = -0.05 \pm 0.20 \pm 0.03$, $\mathcal{A}_{CP}(B^\pm \to \phi K^{*\pm}) = -0.43 \,^{+\,0.36}_{-\,0.30} \pm 0.06$, and $\mathcal{A}_{CP}(\overset{(-)}{B}{}^0 \to \phi \overset{(-)}{K}{}^{*0}) = 0.00 \pm 0.27 \pm 0.03$.

PACS numbers: 13.25.Hw, 11.30.Er, 14.40.Nd

The phenomenon of Charge-Parity (CP) symmetry violation has played an important role in understanding fundamental physics since its initial discovery in the K meson system in 1964 [1]. Soon after, it was recognized that the violation of CP symmetry was one of the fundamental requirements to produce a matter-dominated Universe [2]. A significant CP-violating asymmetry in decays of neutral B mesons to final states containing charmonium, due to interference between $B^0 - \overline{B}{}^0$ mixing and direct decay amplitudes, has recently been observed [3]. As it has now been established [4] that the CP-violating decays of the K_L^0 meson to $\pi\pi$ final states are due to CP violation in decay amplitudes as well as to $K^0 - \overline{K}{}^0$ mixing, it is topical to search for "direct" CP asymmetries in B decays, which involve only direct decay amplitudes. These asymmetries are anticipated to be much larger in B decays than in K decays [5]. Direct CP violation would be measured as an asymmetry of B decay rates:

$$\mathcal{A}_{CP} \equiv \frac{\Gamma(\overline{B} \to \bar{f}) - \Gamma(B \to f)}{\Gamma(\overline{B} \to \bar{f}) + \Gamma(B \to f)} \; . \tag{1}$$

Charmless B meson decays are particularly interesting processes to search for direct CP violation because of the possible involvement of penguin (P) and tree (T) amplitudes of comparable magnitude. Substantial CP violation can thus arise in the Standard Model through interference of these terms [5]:

$$\mathcal{A}_{CP} = \frac{2\;|P|\;|T|\;\sin\Delta\phi\;\sin\Delta\delta}{|P|^2 + |T|^2 + 2\;|P|\;|T|\;\cos\Delta\phi\;\cos\Delta\delta}\;, \tag{2}$$

where $\Delta\phi$ and $\Delta\delta$ are the differences in weak and strong phases. Because of the weak phase difference between the tree and penguin amplitudes, $\mathcal{A}_{CP}$ is sensitive to the Cabibbo-Kobayashi-Maskawa matrix [6] phases $\gamma \equiv \arg\left[\,-V_{ud}V_{ub}^* \,/\, V_{cd}V_{cb}^*\,\right]$ and $\alpha \equiv \arg\left[\,-V_{td}V_{tb}^* \,/\, V_{ud}V_{ub}^*\,\right]$. The difference between the $b \to u$ tree and $b \to s$ ($b \to d$) penguin amplitude weak phases $\Delta\phi$ is γ (α), as in the case of the decays $B \to \pi K$, $\eta' K$ ($B \to \pi\pi$, $\omega\pi$). However, large uncertainties in the strong phases, which can be calculated by certain models, weakens the quantitative relationship to the weak phases. Recent calculations based on effective theory and factorization predict asymmetries as large as $\sim$10% [7].

The measurement of direct CP violation in pure penguin modes, such as $B \to \phi K^{(*)}$, is more sensitive to non-Standard-Model physics. In the Standard Model, the lack of a tree-level contribution results in an expected $\mathcal{A}_{CP}$ of no more than $\sim$1% [7]. However, new particles in loops, such as charged Higgs boson or SUSY particles, would provide additional amplitudes with different phases. Depending on the model parameters, $\mathcal{A}_{CP}$ can be 30% or larger in such scenarios [8]. Complementary searches for new physics would involve measurements of the time-dependent asymmetries in $\overset{(-)}{B}{}^0$ decays to CP eigenstates, such as $\eta' K^0_{S(L)}$, $\phi K^0_{S(L)}$, and $\phi \overset{(-)}{K}{}^{*0} (\to K^0_S \pi^0)$. Comparison of the value of $\sin 2\beta$ obtained from these modes with that from charmonium modes [3] can probe for new physics participating in penguin loops. In these measurements, direct CP violation in the decay becomes highly relevant and can be studied in the self-tagging modes discussed below.

The CLEO experiment has reported a search for direct CP violation in B meson decays to πK, $\eta' K$, and $\omega\pi$ [9]. In this paper we improve the precision of the measurements in the $\eta' K$ and $\omega\pi$ modes and extend the search to new modes. Measurements from *BABAR* of the $B \to \pi K$ charge asymmetries are presented elsewhere [10, 11]. Here we present measurements of the charge asymmetries in the following charmless B decays, for which branching fractions have been previously reported [12, 13]: $B^\pm \to \eta' K^\pm$, $B^\pm \to \omega\pi^\pm$, $B^\pm \to \phi K^\pm$, $B^\pm \to \phi K^{*\pm}$, and $\overset{(-)}{B}{}^0 \to \phi \overset{(-)}{K}{}^{*0}$. The B flavor is determined by its charge, except for the $\phi \overset{(-)}{K}{}^{*0}$ final state where the flavor is determined from the charge of the kaon from the $\overset{(-)}{K}{}^{*0} \to K^\pm \pi^\mp$ decay.

The data were collected with the *BABAR* detector [14] at the PEP-II asymmetric-energy e^+e^- collider [15] located at the Stanford Linear Accelerator Center. The results presented in this paper are based on data taken in the 1999–2000 run comprising an integrated luminosity of 20.7 fb^{-1}, corresponding to 22.7 million $B\overline{B}$ pairs, at the $\Upsilon(4S)$ resonance ("on-resonance") and 2.6 fb^{-1} approximately 40 MeV below this energy ("off-resonance"). The $\Upsilon(4S)$ resonance occurs at the e^+e^- center-of-mass (c.m.) energy, $\sqrt{s}$, of 10.58 GeV.

Charged particles are tracked and their momenta measured with a combination of a silicon vertex tracker (SVT) consisting of five double-sided detectors and a 40-layer central drift chamber (DCH), both operating in a 1.5 T solenoidal magnetic field. With the SVT, a position resolution near the interaction point of about 40 μm is achieved for the highest momentum charged particles, allowing the precise determination of decay vertices. The tracking system covers 92% of the solid angle in the c.m. frame. The track finding efficiency is on average (98±1)% for momenta above 0.2 GeV/c and polar angles greater than 500 mrad. Photons are detected by a CsI(Tl) electromagnetic calorimeter (EMC), which provides excellent angular and energy resolution with high efficiency for energies above 20 MeV [14]. The energy resolution of the EMC is 3% and the angular resolution is 4 mrad for photons of energy 1 GeV.

The asymmetric beam configuration in the laboratory frame provides a boost to the $\Upsilon(4S)$ increasing the momentum range of the B meson decay products up to 4.3 GeV/c. Charged particle identification is provided by the average energy loss (dE/dx) in the tracking devices and by an internally reflecting ring imaging Cherenkov detector (DIRC) covering the central region. A K–π separation of better than four standard deviations (σ) is achieved for momenta below 3 GeV/c, decreasing to 2.5σ at the highest momenta in our final states. Electrons are identified by the tracking system and the EMC.

Hadronic events are selected based on track multiplicity and event topology. We reconstruct B meson candidates from their charged and neutral decay products, including the intermediate states $\eta' \to \eta\pi^+\pi^-$ ($\eta'_{\eta\pi\pi}$) or $\rho^0\gamma$ ($\eta'_{\rho\gamma}$), $\omega \to \pi^+\pi^-\pi^0$, $\phi \to K^+K^-$, $K^{*\pm} \to \overset{(-)}{K}{}^0\pi^\pm$ ($K^{*\pm}_{K^0}$) or $K^\pm\pi^0$ ($K^{*\pm}_{K^+}$), $\overset{(-)}{K}{}^{*0} \to K^\pm\pi^\mp$, $\rho^0 \to \pi^+\pi^-$, $\pi^0 \to \gamma\gamma$, $\eta \to \gamma\gamma$, and $\overset{(-)}{K}{}^0 \to K^0_S \to \pi^+\pi^-$. The selection requirements are identical to those used in the branching fraction measurements [12, 13].

Candidate charged tracks are required to originate from the interaction point, and to have at least 12 DCH hits and a minimum transverse momentum of 0.1 GeV/c. Looser criteria are applied to tracks forming K^0_S candidates to allow for displaced decay vertices. Kaon tracks are distinguished from pion and proton tracks via a likelihood ratio that includes dE/dx information from the SVT and DCH, and, for momenta above 0.7 GeV/c, the Cherenkov angle and number of photons as measured by the DIRC.

We form K^0_S, ϕ, $\overset{(-)}{K}{}^{*0}$, and ρ^0 candidates from pairs of oppositely charged tracks that form a consistent vertex. We further combine a pair of charged tracks with a consistent vertex and a π^0 or η candidate to select ω or $\eta'_{\eta\pi\pi}$ candidates. The K^0_S candidates are required to satisfy $|m(\pi^+\pi^-) - m_{K^0}| < 12$ MeV/c^2 with the cosine of the angle between their reconstructed flight and momentum directions greater than 0.995 and the measured proper decay time greater than three times its uncertainty.

We reconstruct π^0 (η) mesons as pairs of photons, each with a minimum energy deposition of 30 MeV (100 MeV) in the EMC. The typical resolution of the reconstructed π^0 mass is 7 MeV/c^2. A ± 15 MeV/c^2 interval centered on the nominal π^0 mass [16] is applied to select π^0 candidates. We combine a ρ^0 candidate with a photon of energy above 200 MeV to obtain an $\eta'_{\rho\gamma}$ candidate.

We select ϕ, ω, η', and η candidates with requirements on the invariant masses (in MeV/c^2) loose enough to retain sidebands for later fitting: $990 < m(K^+K^-) < 1050$, $735 < m(\pi^+\pi^-\pi^0) < 830$, $930 < m(\eta\pi^+\pi^-) < 990$, $900 < m(\rho\gamma) < 1000$, and $490 < m(\gamma\gamma) < 600$. The experimental resolutions in the K^* and ρ invariant masses are negligible with respect to their natural widths. The $K\pi$ invariant mass interval is ± 150 MeV/c^2 for the charged and ± 100 MeV/c^2 for the neutral K^* candidates. We require the invariant mass of ρ candidates to be between 500 and 995 MeV/c^2.

The helicity angle θ_H of a ϕ, K^*, or ω resonance is defined as the angle between the direction of one of two daughters, or the normal to the ω decay plane, and the parent B direction in the resonance rest frame. To suppress combinatorial background, we require the cosine of the $K^{*\pm} \to K^\pm\pi^0$ helicity angle, defined with respect to the kaon, to be greater than -0.5. This effectively requires the π^0 momentum to be above 0.35 GeV/c.

We identify B meson candidates kinematically using two nearly independent variables [14], the energy-substituted mass $m_{\rm ES} = [(s/2 + \mathbf{p}_i \cdot \mathbf{p}_B)^2/E_i^2 - \mathbf{p}_B^2]^{1/2}$ and $\Delta E = (E_iE_B - \mathbf{p}_i \cdot \mathbf{p}_B - s/2)/\sqrt{s}$, where $(E_i, \mathbf{p}_i)$ is the initial state four-momentum, obtained from the beam momenta, and $(E_B, \mathbf{p}_B)$ is the four-momentum of the reconstructed B candidate. A quantity that is almost equivalent to $m_{\rm ES}$ can be obtained from a kinematic fit of the measured candidate four-momentum in the $\Upsilon(4S)$ frame with its energy constrained to that of the beam [13]. For signal events ΔE peaks at zero and $m_{\rm ES}$ at the B mass. Our initial selection requires $m_{\rm ES} > 5.2$ GeV/c^2 and $|\Delta E| < 0.2$ GeV.

Charmless hadronic modes suffer from large background due to random combinations of tracks produced in the quark-antiquark continuum ($e^+e^- \to q\bar{q}$). This background is distinguished by its jet structure as compared to the spherical decays of the B mesons produced in the $\Upsilon(4S)$ decays. To reject continuum background we make use of the angle θ_T between the thrust axis of the B candidate and that of the rest of the tracks and neutral clusters in the event, calculated in the c.m. frame. The distribution of $\cos\theta_T$ is sharply peaked near ± 1 for combinations drawn from jet-like $q\bar{q}$ pairs, and nearly uniform for the isotropic B meson decays. Thus we require $|\cos\theta_T| < 0.9$ (0.8 for $\phi K^{*\pm}$). We also construct a Fisher discriminant that combines eleven variables [17]: the polar angles of the B momentum vector and the B-candidate thrust axis with respect to the beam axis in the $\Upsilon(4S)$ frame, and the scalar sum of the c.m. momenta of charged particles and photon (excluding particles from the B candidate) entering nine 10° polar angle intervals coaxial around the B-candidate thrust axis. Monte Carlo (MC) simulation [18] demonstrates that contamination from other B decays is negligible.

We use an unbinned extended maximum likelihood (ML) fit to extract signal yields and charge asymmetries simultaneously. The extended likelihood for a sample of N events is

$$\mathcal{L} = \exp\left(-\sum_{i,k} n_{ik}\right) \prod_{j=1}^{N} \left(\sum_{i,k} n_{ik}\, \mathcal{P}_{ik}(\vec{x}_j; \vec{\alpha})\right), \qquad (3)$$

where $\mathcal{P}_{ik}(\vec{x}_j; \vec{\alpha})$ is the probability density function (PDF) for measured variables $\vec{x}_j$ of an event j in category i and flavor state k, and n_{ik} are the yields extracted from the fit. The fixed parameters $\vec{\alpha}$ describe the expected distributions of measured variables in each category and flavor state. The PDFs are non-zero only for the correct final state flavor ($k = 1$ for $\overline{B} \to \bar{f}$ and $k = 2$ for $B \to f$). In the simplest case, there are two categories, signal and background ($i = 1, 2$). The decays with the charged primary daughter $B^\pm \to X^0h^\pm$ ($h^\pm = K^\pm$ or $\pi^\pm$, and $X^0 = \eta'$, ω, or ϕ) are fit simultaneously with two signal ($i = 1$ for $B^\pm \to X^0K^\pm$ and $i = 2$ for $B^\pm \to X^0\pi^\pm$) and two corresponding background ($i = 3, 4$) categories.

We rewrite the event yields n_{ik} in each category in terms of the asymmetry $\mathcal{A}_i$ and the total event yield n_i: $n_{i1} = n_i \times (1 + \mathcal{A}_i)/2$ and $n_{i2} = n_i \times (1 - \mathcal{A}_i)/2$. The event yields n_i and asymmetries $\mathcal{A}_i$ in each category are obtained by maximizing $\mathcal{L}$ [19]. The dependence of $\mathcal{L}$ on a fit parameter n_i or $\mathcal{A}_i$ is obtained with the other fit parameters floating. We quote statistical errors corresponding to unit changes in the quantity $\chi^2 \equiv -2\ln(\mathcal{L}/\mathcal{L}_{\rm max})$, where $\mathcal{L}_{\rm max}$ is the maximum value of the likelihood. The 90% confidence level (C.L.) limits correspond to a change in the χ^2 of 2.69. When more than one channel is measured for the same primary B decay, the channels are combined by adding their χ^2 distributions.

The PDF $\mathcal{P}_{ik}(\vec{x}_j;\vec{\alpha})$ for a given event j is the product of PDFs in each of the independent fit input variables $\vec{x}_j$. These are ΔE, $m_{\rm ES}$, invariant masses of intermediate states (η', ω, ϕ, K^*, and η), Fisher discriminant, and the ϕ and ω helicity angles for pseudoscalar-vector decays. For the simultaneous fit to the decays with the charged primary daughter $h^\pm$ ($B^\pm \to X^0 K^\pm$ and $X^0\pi^\pm$) we include normalized residuals derived from the difference between measured and expected DIRC Cherenkov angles for the $h^\pm$. Additional separation between the two final states is provided by ΔE. The separation depends on the momentum of the charged primary daughter in the laboratory and is about 45 MeV on average varying from about 30 MeV for the highest momentum to about 80 MeV for the lowest momentum primary daughters in our final states.

For the parameterization of the PDFs for ΔE, $m_{\rm ES}$, and resonance masses we employ Gaussian and Breit-Wigner functions to describe the signal distributions. For the background we use low-degree polynomials or, in the case of $m_{\rm ES}$, an empirical phase-space function [20]. The background parameterizations for resonance masses also include a resonant component to account for resonance production in the continuum. In the B decays to vector-vector states, the helicity angle distribution is the result of an *a priori* unknown superposition of transverse and longitudinal polarizations, and thus is not used for background suppression in the fit. For pseudoscalar-vector B decay modes, angular momentum conservation results in a $\cos^2\theta_H$ distribution for signal. The background shape is again separated into contributions from combinatoric background and from real mesons, both fit by nearly constant low-degree polynomials. The Cherenkov angle residual PDFs are Gaussian for both the pion and kaon distributions. The Fisher discriminant is described by an asymmetric Gaussian for both signal and background.

TABLE I: Results of the ML fits, including number of signal events ($n_{\rm sig}$), their charge asymmetry ($\mathcal{A}_{CP}$), and asymmetry 90% C.L. limits. All results include systematic errors, which are quoted second after statistical errors for $n_{\rm sig}$ and $\mathcal{A}_{CP}$.

Mode	$n_{\rm sig}$	$\mathcal{A}_{CP}$	90% C.L.
$\eta' K^\pm$		$-0.11 \pm 0.11 \pm 0.02$	[–0.28,+0.07]
$\eta'_{\eta\pi\pi} K^\pm$	$49.5\ ^{+\ 8.1}_{-\ 7.3} \pm 1.5$	$-0.17 \pm 0.15 \pm 0.01$	
$\eta'_{\rho\gamma} K^\pm$	$87.6\ ^{+13.4}_{-12.5} \pm 3.7$	$-0.05 \pm 0.15 \pm 0.03$	
$\omega\pi^\pm$	$27.6\ ^{+\ 8.8}_{-\ 7.7} \pm 1.9$	$-0.01\ ^{+\ 0.29}_{-\ 0.31} \pm 0.03$	[–0.50,+0.46]
$\phi K^\pm$	$31.4\ ^{+\ 6.7}_{-\ 5.9} \pm 2.3$	$-0.05 \pm 0.20 \pm 0.03$	[–0.37,+0.28]
$\phi K^{*\pm}$		$-0.43\ ^{+\ 0.36}_{-\ 0.30} \pm 0.06$	[–0.88,+0.18]
$\phi K^{*\pm}_{K^0}$	$4.4\ ^{+\ 2.7}_{-\ 2.0} \pm 0.4$	$-0.55\ ^{+\ 0.51}_{-\ 0.35} \pm 0.05$	
$\phi K^{*\pm}_{K^+}$	$7.1\ ^{+\ 4.3}_{-\ 3.4} \pm 1.2$	$-0.31\ ^{+\ 0.54}_{-\ 0.43}\ ^{+\ 0.10}_{-\ 0.06}$	
$\phi \overset{(-)}{K}{}^{*0}$	$20.8\ ^{+\ 5.9}_{-\ 5.1} \pm 1.3$	$0.00 \pm 0.27 \pm 0.03$	[–0.44,+0.44]

The fixed parameters $\vec{\alpha}$ describing the PDFs are extracted from signal and background distributions from MC simulation, on-resonance ΔE and $m_{\rm ES}$ sidebands, and off-resonance data. The MC resolutions in ΔE and $m_{\rm ES}$ are adjusted by comparisons of data and simulation in abundant calibration channels with similar kinematics and topology, such as $B \to D\pi, D\rho$ with $D \to K\pi, K\pi\pi$. The resolutions in the invariant masses of intermediate states are obtained from inclusive particle samples. The simulation reproduces the event-shape variable distributions found in data. The Cherenkov angle residual parameterizations are determined from samples of $\overset{(-)}{D}{}^0 \to K^\mp\pi^\pm$ originating from $D^{*\pm}$ decays.

The results of our ML fit analyses are summarized in Table I. The signal yields along with branching fraction results have been reported earlier [12, 13]. In all cases we find signal event yields with significances, including systematic uncertainties, of greater than four standard deviations, and hence proceed with asymmetry measurements. The measured likelihood values are well reproduced with generated samples. The dependence of the χ^2 on $\mathcal{A}_{CP}$ for each decay mode is shown in Fig. 1 and asymmetry measurements are summarized in Fig. 2. We see no significant asymmetries and determine 90% C.L. intervals.

In the charge asymmetry measurements, systematic uncertainties relevant to branching fraction measurements tend to cancel, but some level of bias is inevitable as neither the *BABAR* detector nor PEP-II is perfectly charge symmetric. However these effects are mostly very small for the final states considered here. Charge biases in track reconstruction and particle identification efficiency have been studied in a sample of more than a billion charged tracks in multi-hadron events. After proton and electron rejection we find an asymmetry in track reconstruction efficiency consistent with zero with an uncertainty of less than 0.01 for a wide range of momenta for tracks originating from the interaction point. Taking into account particle identification requirements similar to the ones applied to the K^* daughters, this consistency is still better than 0.02. A $D^{*\pm}$ control sample of kaon and pion tracks is used to estimate systematic uncertainties in the asymmetries arising from possible charge biases in the Cherenkov angle residual, which are found to be less than 0.01.

From these studies we assign a systematic uncertainty

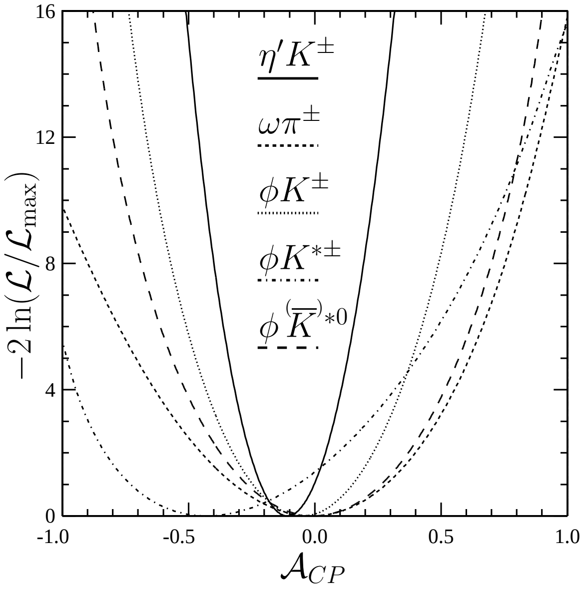

FIG. 1: Dependence of $\chi^2 \equiv -2\ln(\mathcal{L}/\mathcal{L}_{\max})$ on $\mathcal{A}_{CP}$ for each of the B decay modes.

of 0.01 on $\mathcal{A}_{CP}$ for all the modes with a charged primary daughter: $B^{\pm} \rightarrow \eta' K^{\pm}$, $\omega\pi^{\pm}$, and $\phi K^{\pm}$. For the modes with a K^* we account for the broader momentum spectrum of the charged daughters and particle identification applied to the kaon candidates with a 0.02 systematic error. All measured background asymmetries in data and signal asymmetries in MC are consistent with zero within statistical uncertainties.

A different type of uncertainty originates in the ML fit from assumptions about the signal and background distributions. In order to derive systematic errors in the event yield and its asymmetry, we vary the PDF parameters with their respective uncertainties. The systematic errors in the asymmetries are found to be 0.02 for $\eta' K^{\pm}$ and $\phi \overset{(-)}{K}{}^{*0}$, 0.03 for $\omega\pi^{\pm}$ and $\phi K^{\pm}$, and 0.06 for $\phi K^{*\pm}$, the latter being dominated by the mode with a π^0. These systematic errors are conservatively estimated and can be improved with a larger data sample.

Uncorrelated (due to PDF variations) and correlated (due to selection requirements) systematic errors are treated separately in the case of multiple decay channels and each is convolved with the likelihood distributions to account for all systematic effects in the result. The asymmetry measurement in the $\overset{(-)}{B}{}^0 \rightarrow \phi \overset{(-)}{K}{}^{*0}$ decay mode is corrected by the inverse dilution factor $1/(1-2w)$, where w, the fraction of doubly misidentified $K\pi$ combinations originating from $\overset{(-)}{K}{}^{*0}$, is $\sim$0.01. The uncertainties in the final results presented in Table I are dominated by statistical errors.

In summary, we have searched for direct CP violation in charmless hadronic B decays observed in the *BABAR* data. The measured charge asymmetries of the B decays into final states $\eta' K^{\pm}$, $\omega\pi^{\pm}$, $\phi K^{\pm}$, $\phi K^{*\pm}$, and $\phi \overset{(-)}{K}{}^{*0}$ are summarized in Table I and Fig. 2. These results, along with the asymmetry measurements in $B \rightarrow \pi K$ modes [10, 11] and in combination with the earlier measurements [9], rule out a significant part of the physical $\mathcal{A}_{CP}$ region, allowing for constraints on new physics models [8], but are not yet of sufficient precision to allow precise comparison with Standard Model predictions [7].

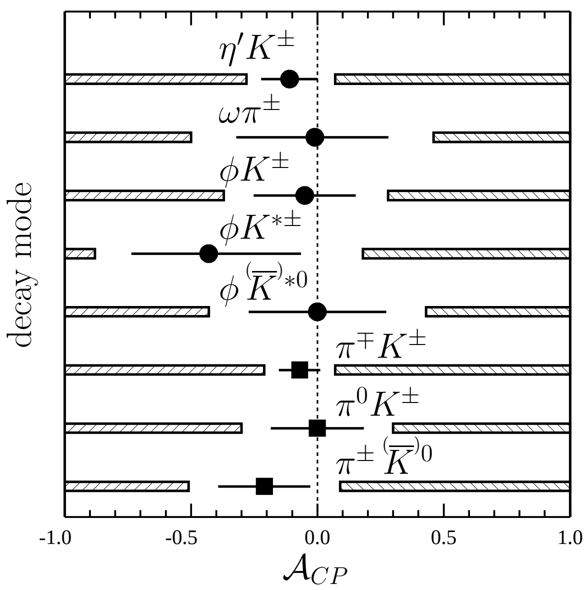

FIG. 2: Results of $\mathcal{A}_{CP}$ measurements for the B decay modes presented in this paper (circles) with the *BABAR* measurements in πK modes (squares) shown for comparison [10, 11]. The data sample for the $\pi^{\mp} K^{\pm}$ result is about 50% larger [11]. Hatched regions are excluded at 90% C.L.

We are grateful for the excellent luminosity and machine conditions provided by our PEP-II colleagues. The collaborating institutions wish to thank SLAC for its support and kind hospitality. This work is supported by DOE and NSF (USA), NSERC (Canada), IHEP (China), CEA and CNRS-IN2P3 (France), BMBF (Germany), INFN (Italy), NFR (Norway), MIST (Russia), and PPARC (United Kingdom). Individuals have received support from the Swiss NSF, A. P. Sloan Foundation, Research Corporation, and Alexander von Humboldt Foundation.

---

[*] Also with Università di Perugia, Perugia, Italy

[†] Also with Università della Basilicata, Potenza, Italy

[1] J. H. Christenson, J. Cronin, V. Fitch, and R. Turlay, Phys. Rev. Lett. **13**, 138 (1964).

[2] A.D. Sakharov, ZhETF Pis'ma **5**, 32 (1967); JETP Lett. **5**, 24 (1967).

[3] *BABAR* Collaboration, B. Aubert *et al.*, Phys. Rev. Lett. **87**, 091801 (2001); BELLE Collaboration, K. Abe *et al.*,

Phys. Rev. Lett. **87**, 091802 (2001).

[4] KTeV Collaboration, A. Alavi-Harati *et al.*, Phys. Rev. Lett. **83**, 22 (1999); NA48 Collaboration, V. Fanti *et al.*, Phys. Lett. B **465**, 335 (1999); NA31 Collaboration, G.D. Barr *et al.*, Phys. Lett. B **317**, 233 (1993).

[5] M. Bander, D. Silverman, and A. Soni, Phys. Rev. Lett. **43**, 242 (1979).

[6] M. Kobayashi and T. Maskawa, Prog. Theor. Phys. **49**, 652 (1973); N. Cabibbo, Phys. Rev. Lett. **10**, 531 (1963).

[7] A. Ali, G. Kramer, and C.-D. Lü, Phys. Rev. D **59**, 014005 (1998); G. Kramer, W.F. Palmer, and H. Simma, Nucl. Phys. B **428**, 77 (1994).

[8] I. Hinchliffe and N. Kersting, Phys. Rev. D **63**, 015003 (2001); X.-G. He, W.-S. Hou, and K.-C. Yang, Phys. Rev. Lett. **81**, 5738 (1998).

[9] CLEO Collaboration, S. Chen *et al.*, Phys. Rev. Lett. **85**, 525 (2000).

[10] *BABAR* Collaboration, B. Aubert *et al.*, Phys. Rev. Lett. **87**, 151802 (2001).

[11] *BABAR* Collaboration, B. Aubert *et al.*, *BABAR*-PUB-01/21, hep-ex/0110062, to appear in Phys. Rev. D.

[12] *BABAR* Collaboration, B. Aubert *et al.*, Phys. Rev. Lett. **87**, 151801 (2001).

[13] *BABAR* Collaboration, B. Aubert *et al.*, Phys. Rev. Lett. **87**, 221802 (2001).

[14] *BABAR* Collaboration, B. Aubert *et al.*, SLAC-PUB-8569, hep-ex/0105044, to appear in Nucl. Instrum. and Methods.

[15] PEP-II Conceptual Design Report, SLAC-R-418 (1993).

[16] Particle Data Group, D.E. Groom *et al.*, Eur. Phys. J. C **15**, 1 (2000).

[17] CLEO Collaboration, D.M. Asner *et al.*, Phys. Rev. D **53**, 1039 (1996).

[18] The *BABAR* detector Monte Carlo simulation is based on GEANT: R. Brun *et al.*, CERN DD/EE/84-1.

[19] F. James, CERN Program Library, D506.

[20] ARGUS Collaboration, H. Albrecht *et al.*, Phys. Lett. B **241**, 278 (1990).